Chemical Papers (2023) 77:6557–6566
https://doi.org/10.1007/s11696-023-02958-2

ORIGINAL PAPER

Bithiophene-naphthalene chalcone as a fluorescent pigment in eco-friendly security ink formulation

Rakshitha K. Jain[1] · Kashmitha Muthamma[1] · Dhanya Sunil[1] · Suresh D. Kulkarni[2] · P. J. Anand[3] · Nilanjan Dey[4]

Received: 16 April 2023 / Accepted: 28 June 2023 / Published online: 7 July 2023

Abstract

Approaches to prevent document/product forgery using eco-friendly printing inks and security printing techniques on flexible substrates are two vital areas of research that demand coherent advancements. In this context, a new bithiophene-naphthalene chalcone (BTNP) was synthesized and characterized as a fluorescent pigment for use in security ink. BTNP exhibited good solid-state and solution phase fluorescence with intramolecular charge transfer confirmed using theoretical studies and emission spectra collected in THF/THF–hexane mixtures. The aggregation-induced emission of BTNP was established using solution phase studies in THF/THF–water mixtures. The strong solid-state yellow emission of BTNP prompted its use as a pigment in the preparation of an environment-friendly UV fluorescent formulation, devoid of any volatile organic compounds or hazardous air pollutants. The screen prints obtained on a UV dull paper substrate utilizing BTNP ink revealed good fluorescence, photostability, colorimetric, densitometric, and rub resistance characteristics, which showcase the potential applicability of the BTNP formulation in security printing. The low cytotoxic nature of the chalcone as observed in the MTT assay could also be exploited for the use of formulation in inkpads.

Graphical abstract

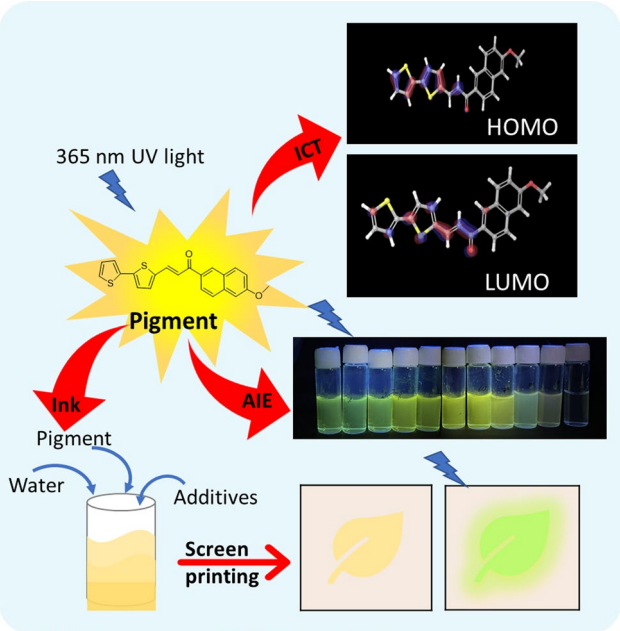

Keywords Bithiophene-naphthalene chalcone · Eco-friendly formulation · UV fluorescent screen prints

Extended author information available on the last page of the article

Introduction

Counterfeiting of security documents, passports, banknotes, and certificates is a significant global problem that costs billions of dollars for businesses, governments, and consumers each year (Pei et al. 2020). To prevent the forgery of documents, there is a need to improve its security features by using high-security anticounterfeiting materials with sophisticated authentication technologies (Abdollahi et al. 2020). Researchers have explored diverse classes of luminescent materials including lanthanides (Li et al. 2021), conventional organic materials (Jeon et al. 2015), plasmonic nanomaterials (Ibrar and Skrabalak 2021), quantum dots (Song et al. 2016), metal–organic frameworks (Mieno et al. 2018; Venkateswarlu et al. 2020), and carbon dots (Jiang et al. 2018) as luminous dyes/pigments for the production of coated papers and security inks in the area of counterfeit prevention. These fluorescent molecules find applications in security printing, wherein they are used as colourants to formulate inks. Recently, short- and long-wavelength UV fluorescent inks are widely applied in security printing arena including smart packaging, highlighting markers, and information storage (Bhagya et al. 2022; Ataeefard and Nourmohammadian 2015). Moreover, due to environmental concerns, there are numerous approaches to create sustainable printing inks such as water-based inks with reduced volatile organic compounds and hazardous air pollutants, rather than using solvent-based inks. These water-based inks have been identified as the best viable option attributed to its environmental friendliness, high solid content, gloss, low viscosity, and so on (Zhou et al. 2015). Therefore, printing industry is now paying close attention to the development of water-based and water-reducible ink formulations to lower the usage of organic solvents that evaporate into the environment (Żołek-Tryznowska et al. 2015).

Certain organic molecules show tunable emission based on their ability to form aggregates that can be used in certain emerging fields (Samanta and Bhattacharya 2012; Gulyani et al. 2018). Chalcones are synthesized through the reaction between aromatic aldehydes and aromatic ketones, and their basic structural framework comprises two aromatic units linked through a three-carbon, α,β-unsaturated ketone system (Ming et al. 2017). The push–pull conjugation effect is primarily responsible for the fluorescent nature of chalcones, and these materials also exhibit good thermal stability that is necessary when utilized in printing applications. The versatile chemistry of thiophene enables the preparation of a wide range of thiophene-based chalcone structures with extremely varied functionalization. Research reports on thiophene oligomers and polymers focus primarily on their semiconductor, luminescence, and sensing capabilities (Barbarella et al. 2005). There are no detailed investigations on the natural colourant bithiophene, which has two coplanar rings and a sulphur atom in each of them as a possible pigment in water-based inks. Low fluorescence emission quantum yields, both in the solution and solid states attributed to an efficient intersystem crossing of heavy sulphur atoms, aggregation-induced quenching, well-aligned packing arrangement in the solid state, and excited state relaxation favoured by inter-annular rotations restricts the usage of bithiophene in optical applications. Despite these limitations, during the past few years, numerous extremely luminous thiophene-based materials with strong fluorescence and quantum yield, as well as high absorption coefficients, have been synthesized for diverse applications (Rasmussen et al. 2015; Wakamiya et al. 2007; Kim and Son 2011);(Lee et al. 2021). Moreover, bithiophene derivatives with intense emissions spanning the entire visible spectral region have been achieved by tuning the electron-donating ability of the π-conjugated framework of bithiophene (Wakamiya et al. 2007).

In the quest for new fluorescent molecules as colourants in water-based ink compositions, naphthalene and 2,2′-bithiophene integrated chalcone (BTNP) with electronic delocalization and push–pull conjugation was synthesized. Further, the structural, optical, and cytotoxicity features of BTNP are investigated. Screen printing can deposit a thin water-based ink film with no chemical usage and thereby reduces eco-footprint (Karuppusamy et al. 2017). During screen printing, the ink is pumped into the frame and poured onto the screen, which is then pressed through the open holes of the screen by drawing it across the mesh with a rubber-bladed squeegee (Leach et al. 1988). The paper substrate is simultaneously kept in touch with the screen to allow the transfer of ink to it. Screen production is attractive for short-run work because they can be made easily and inexpensively (Leach et al. 1988). Therefore, an environmentally benign water-based formulation for screen printing was prepared using BTNP as the fluorescent pigment. Instant prints obtained with good optical and abrasion resistance characteristics may possibly be applied in a variety of anticounterfeit applications.

Experimental section

Synthesis and characterization of (*E*)-3-([2,2'-bithiophen]-5-yl)-1-(6-methoxynaphthalen-2-yl) prop-2-en-1-one (BTNP)

NaOH solution (10%, 1 mL) was added dropwise into 6-methoxy-2-acetonaphthone (Sigma-Aldrich; 2 mmol) dissolved in ethanol with continuous stirring. Ethanolic solution of 2,2-bithiophene-5-carboxaldehyde (Sigma-Aldrich;

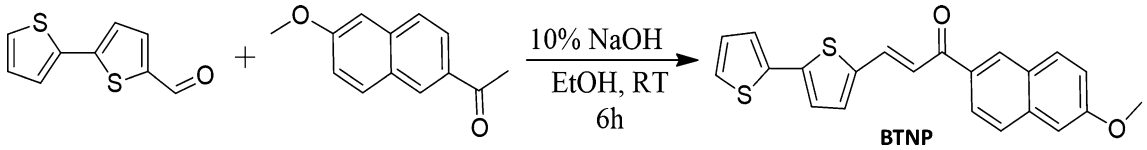

Scheme 1 Synthetic route of BTNP

2 mmol) was added, and the reaction mixture was further stirred at room temperature (RT) for 6 h. The precipitate was filtered, washed with ethanol, dried, and recrystallized using ethanol. Scheme 1 depicts the synthetic route for BTNP.

The open capillary method was used to check the melting point of BTNP. The FTIR, NMR, and mass spectra were obtained using ATR Shimadzu-IR Spirit analyser, 400-MHz Bruker spectrometer, and Agilent 6430 Triple Quad instrument (electrospray ionization), respectively. The absorption and emission studies were performed using 1800 Shimadzu UV–visible spectrophotometer and JASCO spectrofluorometer FP 8300 instruments.

(*E*)-3-([2,2'-bithiophen]-5-yl)-1-(6-methoxynaphthalen-2-yl)prop-2-en-1-one (BTNP): mustard yellow (89%); m.p: 144–146 ℃; FTIR (cm^{-1}): 3071 (Ar. C-H *str.*), 2968, 2833 (aliphatic C-H *str.*), 1651 (C = O *str.*), 1614 (C = C *str.*), 1475, 1436, 1227, 1032 (Thiophene *str.*), (Supplementary Figure S1); ^{1}H NMR (400 MHz, $CDCl_3$, ppm): δ 3.899 (s, 3H), 7.000 (s, 1H), 7.111–7.228 (m, 6H), 7.369–7.407 (d, 1H, 15.2 Hz), 7.743–7.765 (d, 1H, 8.8 Hz), 7.832–7.854 (d, 1H, 8.8 Hz), 7.869–7.906 (d, 1H, 14.8 Hz), 8.005–8.026 (d, 1H, 8.4 Hz), 8.406 (s, 1H), (Fig. S2); ^{13}C (100 MHz, $CDCl_3$, ppm): δ 187.99, 158.72, 139.55, 138.17, 136.19, 135.77, 135.57, 132.51, 132.33, 130.15, 128.71, 127.13, 126.90, 126.26, 124.74, 124.13, 123.84, 123.59, 119.29, 118.71, 104.79, 54.43 (Fig. S3) MS $C_{22}H_{16}O_2S_2$ (*m/z*): M + 1 = 377.0499 (Fig. S4).

Cell culture and cell viability assay

About 1×10^5 cells were seeded per well in a 96-well plate and incubated for 24 h at 37 °C in humidified 5% CO_2 incubator (Sanyo, UK). The cells were treated with different concentrations of BTNP and incubated for 24 h. Further, the cells were washed, and 50 µL of MTT (2 mg/mL) was added and incubated in the dark for another 3 h. Finally, the entire medium was removed from the wells, incubated for 15 min in the dark after adding 50-µL DMSO, and the absorbance was measured at 540 nm. The percentage of viable cells was calculated using Eq. (1).

$$\% \text{ Cell viability} = \frac{\text{Test absorbance} - \text{Blank absorbance}}{\text{Vehicle control absorbance} - \text{Blank absorbance}} \times 100 \quad (1)$$

Ink preparation and evaluation of print properties

The ink components including solvents, acrylic emulsions, and additives were purchased from BASF Chemicals, DOW Chemical Company, Kamson's Pvt. Ltd., and Evonik Industries. Initially, the ink concentrate was prepared by milling a mixture (wt %) of BTNP (13.14), acrylic emulsion 1 (73.56), wetting and dispersing agent (1.59), and ethyl carbitol (11.71) in the Lloyd pigment Muller. Further, the remaining constituents were added and dispersed to attain the final formulation having the following composition (wt %): pigment BTNP (7.49), acrylic emulsion 1 (53.34), Vicoat-1077 (21.39), wax (Joncryl; 2.36), de-foamer (BYK-022; 1.97), wetting and dispersing agent (0.91), ethyl carbitol (6.68), water (2.45), and 25% ammonia solution (3.41). Hegman gauge was utilized to determine the particle size of the BTNP formulation.

The coatings and screen prints were obtained on UV dull paper substrates procured from Manipal Press Pvt. Ltd., Manipal, India. A 120SS mesh screen was used for printing. The photostability of the deposited BTNP ink film was studied by subjecting the screen prints for different durations under UV light of 20 W. Sutherland ink rub tester was utilized to perform the rub test by laying the printed substrate against the blank substrate on the test rubber pad (4 lbs). Xrite I1 Pro spectrophotometer was used to check the colorimetric data. The values of CIELAB colour coordinates: lightness (L*) ranging from 0 (black) to 100 (white), a* (green for negative and red for positive), and b* (blue for negative and yellow for positive) extending from -120 to 120 were explored. The colour differences (ΔE) were calculated using Eq. 2 (Żołek-Tryznowska et al. 2015; Muthamma et al. 2021).

$$\Delta E = \sqrt{(\Delta L^*)^2 + (\Delta a^*)^2 + (\Delta b^*)^2} \quad (2)$$

where $(\Delta L^*) = L^*_{(u)} - L^*$; $(\Delta a^*) = a^*_{(u)} - a^*$; $(\Delta b) = b^*_{(u)} - b^*$ are the variations between the screen printed, and *(u)* is the blank/unprinted paper samples (Żołek-Tryznowska et al. 2015). The surface morphologies of the blank and screen-printed samples were imaged using INNOVA SPM atomic force (AFM) and Carl Zeiss EVO 18 analytical scanning electron microscopes (SEM).

Results and discussion

The chalcone BTNP was synthesized via a base-catalyzed Claisen–Schmidt condensation reaction.

Structural characterization of BTNP

The spectral characterization data obtained were in accordance with the molecular structure of BTNP. The characteristic peaks for C=O and C=C in IR spectrum of the chalcone were obtained at 1651 cm^{-1} and 1570 cm^{-1}, respectively. The ^{1}H NMR spectrum displayed the methoxy protons at 3.8 ppm and the aromatic protons around 7.0–8.4 ppm. The aliphatic carbon and the carbon of the carbonyl group appeared at 54.43 and 187.99 ppm in the $^{13}CNMR$ spectrum, and the mass spectrum was in agreement with the structure of BTNP.

Optical features of BTNP

To get insights into the optical characteristics of the chalcone, its electronic spectral traces were examined. The absorption spectrum of BTNP dissolved in THF (1×10^{-5} M) as presented in Fig. S5 exhibited two absorption peaks at 329 and 406 nm owing to the transitions of the conjugated structural framework as well as π-π^* and n-π^* transitions (Al-Ansari 2016; Omar et al. 2018). The emission spectrum of solid BTNP was recorded (Fig. 1a) to comprehend the fluorescence features for its use as a colourant in water-based ink. BTNP strongly emits at 545 nm, which corresponds to yellowish–green fluorescence as observed from the chromaticity diagram presented in Fig. 1b ($\lambda_{ex}=490$ nm). The sensitivity of BTNP to general solvents helps in analysing its solution phase emission characteristics. The emission spectrum of BTNP dissolved in THF (1×10^{-4} M) was recorded upon excitation at 360 and 440 nm and is portrayed in Fig. 1c, which shows two distinct peaks at around 490

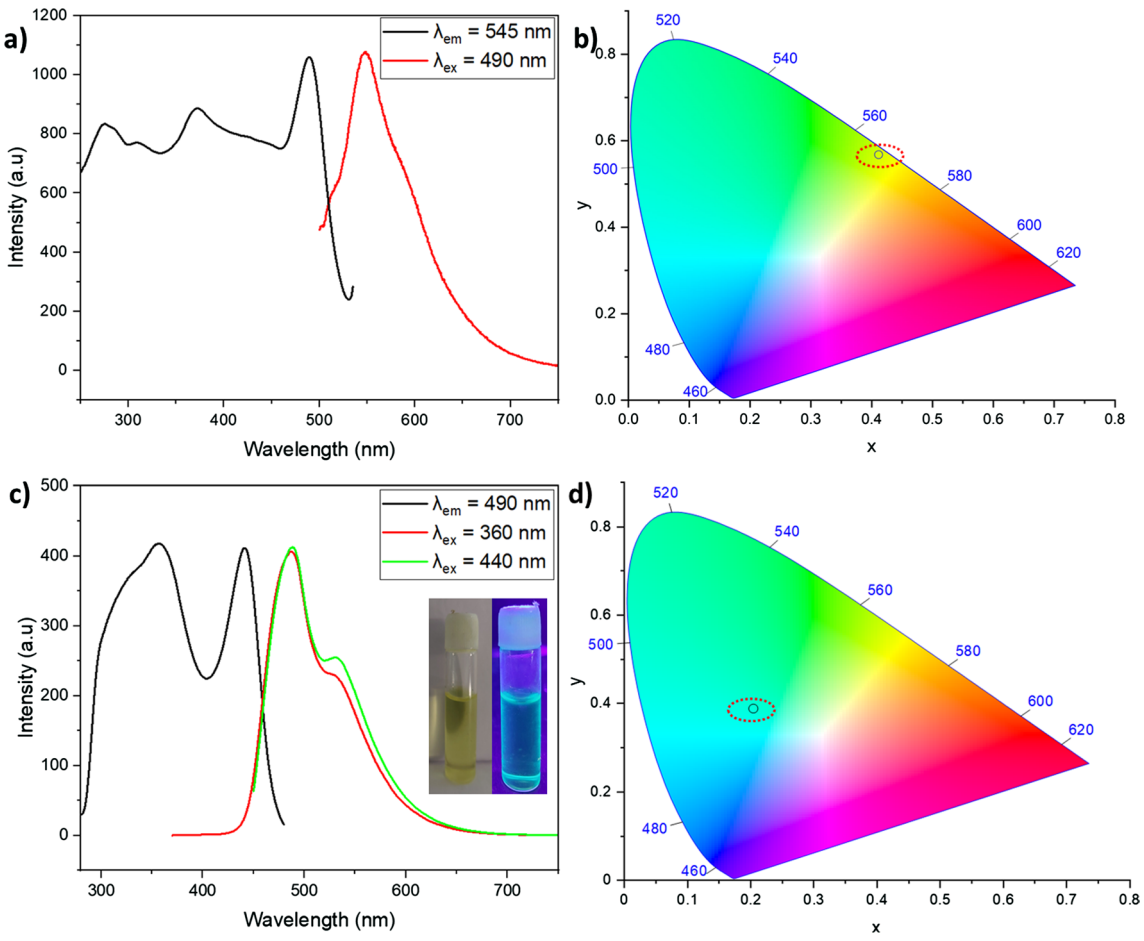

Fig. 1 BTNP in solid state: **a** excitation and emission spectra and **b** corresponding CIE plot. BTNP in THF (1×10^{-4} M): **c** emission and excitation spectra and **d** corresponding CIE plot

and 530 nm indicating a cyan fluorescence as observed from the corresponding chromaticity diagram in Fig. 1d.

When fluorophores are subjected to change in solvent polarity, emission peaks may shift mainly due to the chemical interactions not only between the reactive domains induced in the surrounding solvent and the dipole moment of the fluorophore, but also between one or more solvent molecules and the fluorophore (Lakowicz 1983). Therefore, to determine the impact of solvent polarity on the fluorescence of BTNP, the emission characteristics in THF/THF–hexane (1×10^{-4} M) mixtures were studied. The respective spectrum as shown in Fig. 2a displays a reduction in the fluorescence intensity together with a hypsochromic shift from 490 to 460 nm, indicating that the molecule under study undergoes an intramolecular charge transfer phenomenon (Sowmiya et al. 2011). The density functional theoretical (DFT) studies were executed to generate the optimal molecular geometry (Fig. 2b), highest occupied (HOMO: Fig. 2c), and lowest unoccupied molecular orbitals (LUMO: Fig. 2d). It is observed that the electron density in HOMO is localized in the bithiophene moiety, whereas the electron cloud is present exclusively on the spacer and thiophene moiety in the LUMO. The energy values calculated for HOMO and LUMO are − 5.294 eV and − 2.281 eV with an optical band gap of 3.013 eV.

The conformation of chalcone with extended π-conjugation is generally responsible for the origin of aggregation-induced emission (AIE) that can result in intensified solid-state emission, which have garnered research focus due to their wide potential applications (Kagatikar and Sunil 2021). Therefore, AIE property of BTNP was studied by recording the emission spectra in THF/THF–water mixtures (1×10^{-4} M) with increasing water percentages from 0 to 99%. The samples were excited at 360 nm, and it is observed from the spectra (Fig. 3a) that 0% water fraction has emission at 490 (major peak) and 530 nm (minor peak). With the increase in water content, fluorescence intensity increases and reaches a maximum at 60% water fraction, whereas the fluorescence peak from 530 nm is shifted to 547 nm with high intensity (emission corresponding to solid-state emission), indicating the aggregate formation. The photographs of the respective solutions in daylight and under 365-nm UV illumination are presented in Fig. 3b.

Cytotoxicity studies

The biocompatibility of BTNP was inspected in Vero cells. The MTT assay demonstrated a low toxicity profile of BTNP in Vero cells at low concentrations. The cell viability plot against the studied BTNP concentration is shown in Fig. 3c.

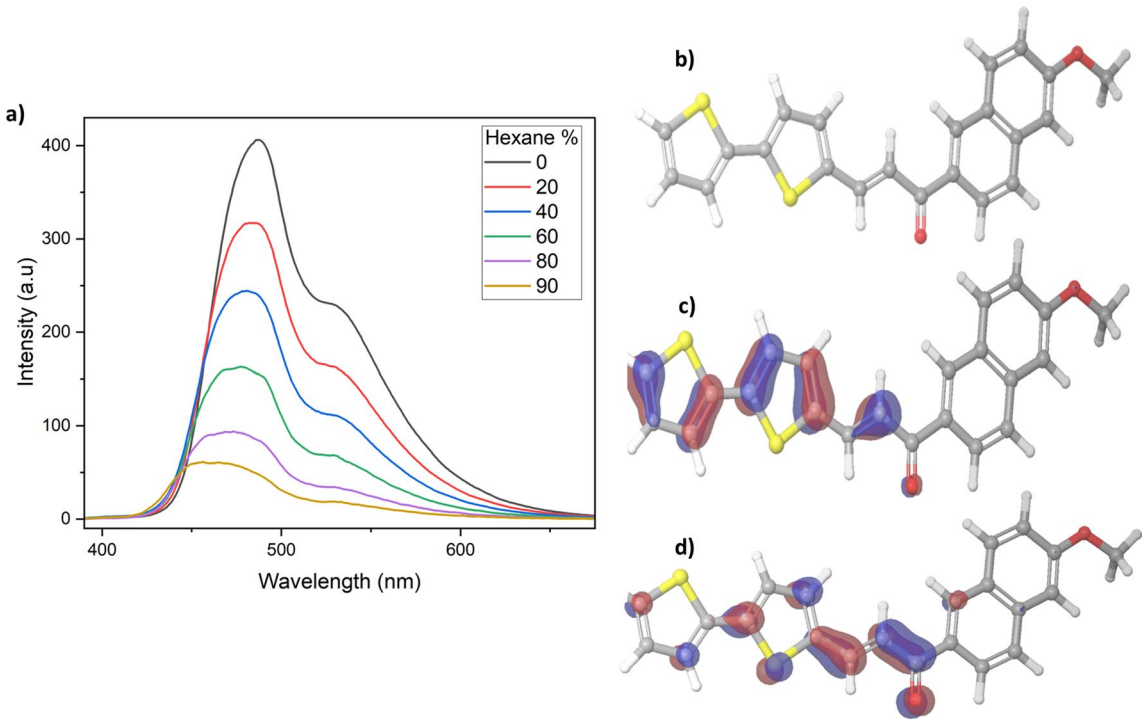

Fig. 2 **a** Fluorescence spectra of BTNP in THF–hexane mixtures with varying hexane fractions (1×10^{-4} M) at λ_{ex}= 360 nm, **b** optimized geometry, **c** HOMO, and **d** LUMO energy levels of BTNP

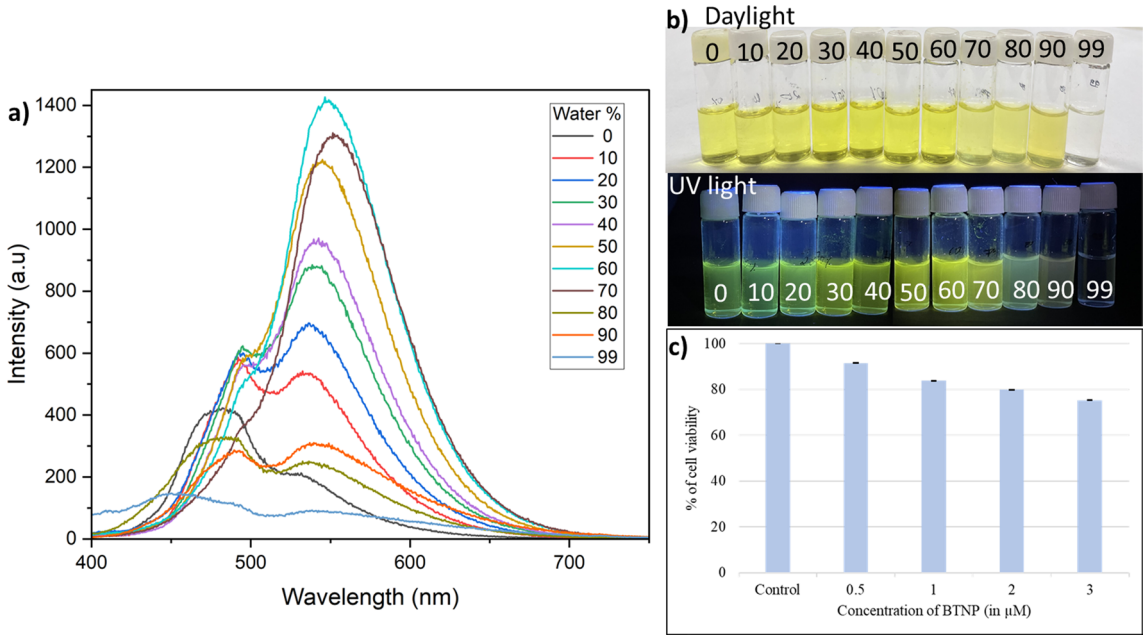

Fig. 3 **a** AIE phenomenon of BTNP in THF–water mixtures with varying water fractions (1×10^{-4} M) at λ_{ex}= 360 nm, **b** photographs of BTNP in THF/THF–water mixtures (from 0 to 99%) in daylight and illumination with 365-nm UV light, and C) MTT assay plot of BTNP

Printing ink features and assessment of screen print properties

Screen printing is mainly used in the printing of fluorescent posters, stickers, display showcards, water-slide transfers, etc. UV fluorescent BTNP was used to prepare a water-based screen-printing ink (Fig. S6), which demonstrated particle size below 10 µm. The carrier/solvent of the ink was primarily water along with other additives, while the pigment BTNP served as the fluorescent colourant as mentioned in the experimental part. The ink displayed bright yellow fluorescence upon illumination with a 365 nm UV light source. Surface interactions between printing ink and the cellulose substrate are vital to obtain an adherent and uniform print. The UV dull paper substrate was initially manually coated with BTNP ink using a zero number bar coater to check the colour mixing and print properties. Further, the fluorescence spectrum (Fig. 4a) collected for the ink-coated paper sample displayed an emission at 543 nm. The chromaticity diagram as portrayed in Fig. 4b indicates that the fluorescence emission from the coated paper sample corresponds to the solid-state fluorescence of BTNP. Moreover, the spectra also provide evidence for the increase in fluorescence emission intensity with rising film thickness (Fig. 4a) upon coating the substrate twice and thrice with the ink. The screen prints obtained using the BTNP formulation on UV dull paper substrate dried immediately at room temperature and showed intense yellowish–green fluorescence under 365 nm UV illumination as presented in Fig. 4c. Further, the corresponding emission was perceived at 543 nm as depicted in Fig. 4d. In addition, the lightfastness of the deposited ink film was probed, wherein the printed samples were exposed to UV light of 20 W for 10–50 min. The emission spectra recorded as depicted in Fig. 4e indicate that the fluorescence intensity of the samples slightly decreased till 30 min of UV exposure and did not show any significant reduction in intensity even up to 50 min of UV exposure, suggesting good lightfastness of the BTNP ink film. The corresponding chromaticity plots (Fig. 4f) also direct towards the good UV stability of the water-based formulation on the flexible porous substrate.

Colorimetric studies of the screen-printed paper samples

The colour coordinates can be determined using basic colorimetric measurements. The International Commission on Illumination (CIE) provides an approach to achieve numbers that measure the sample colour as observed under a standard illumination source. The L*, a*, and b* values for the coated and screen-printed samples specify that with an increase in the number of coatings (C1-C3), the b* value increases and is greater than a* indicating the dominance of yellow colour. The increasing ΔE value for the coated samples indicates that the colour becomes brighter. The colour alterations of the screen prints after UV exposure and rub test were measured using CIELAB colour space and are listed in Table 1. Although the b* value is greater than a*, with increasing UV exposure, there is a decrease in b* and ΔE values, which

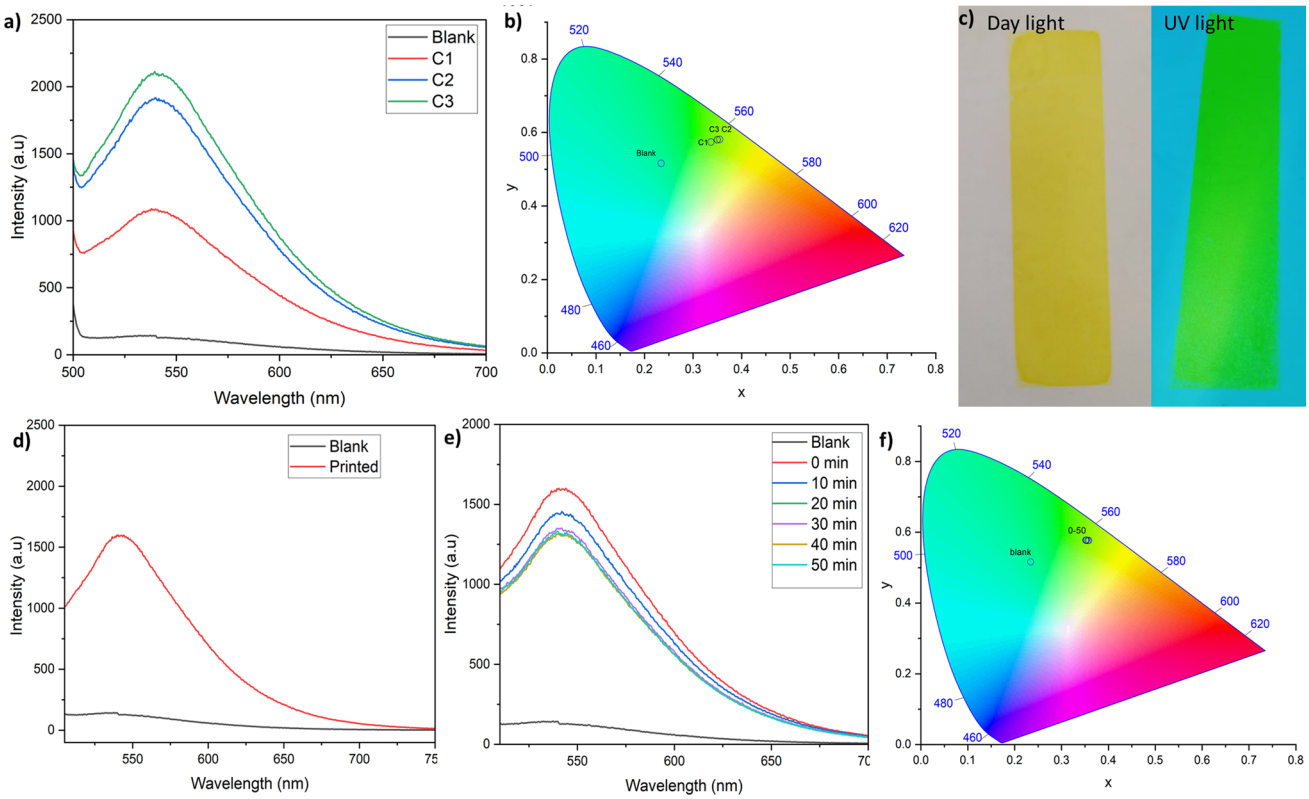

Fig. 4 **a** Emission spectra and **b** respective chromaticity diagram of ink-coated paper sample, **c** photographs of the screen-printed sample under daylight and UV light, **d** emission spectra of screen-printed sample, and **e** emission spectra and **f** respective chromaticity diagram of screen prints exposed to UV light

Table 1 Comparison of colorimetric values of coated and screen-printed paper samples

	L	a	b	ΔE	Density
Reference	90.5	0.36	5.32	–	90.5
Blank	89.94	0.46	4.62	0.90	0.04
Coated and printed samples					
C1	89.1	−6.56	41.21	36.57	0.32
C2	88.39	−6.65	58.45	53.63	0.43
C3	86.83	−4.38	74.08	69.02	0.46
P1	87.12	−5.8	61.38	56.49	0.52
Lightfastness test (UV exposure time in minutes)					
0	86.61	−5.94	60.47	56.43	0.5
10	86.23	−5.96	59.69	55.68	0.5
20	87.47	−6.3	59.02	54.99	0.48
30	86.13	−6.01	59.39	55.40	0.51
40	87.21	−6.2	59.25	55.22	0.49
50	87.21	−6.4	57.65	53.66	0.48
Rub test (no. of rubs)					
0	88.61	−5.9	58.55	54.12238	0.47
25	89.21	−5.93	59.48	55.02778	0.46
50	88.59	−5.88	58.92	54.48789	0.47
75	87.32	−5.48	61.77	57.33655	0.48
100	87.34	−5.68	60.85	56.44403	0.46

signifies that the colour brightness is decreasing. The rub test for determining scratch resistance was created to replicate the kind of impairment that would happen from rubbing paper against a printed image (Mortimer and Varley 2011). The resistance of the ink film printed on paper to abrasion was checked by examining the colorimetric values of the prints after subjecting them to 25, 50, 75, and 100 strokes. The minor changes in the colorimetric values and ΔE values after the rub test compared to 0 rubbed sample vividly prove the good rub resistance of the screen-printed ink film on the flexible paper substrate.

The introduction of 6-methoxynaphthalene moiety into the bithiophene chalcone framework rather than 4-fluorophenyl (BTCF) as in our earlier report (Muthamma et al. 2023) has brought in more intense emission due to extension in the delocalization of electrons. The screen print proofs obtained using BTNP ink displayed superior features compared to the BTCF ink film obtained on the paper substrate using flexography. Though the print properties of the ink films obtained through screen and flexo printing processes cannot be directly compared, generally the BTNP ink film was found to be superior in terms of lightfastness and rub resistance.

Surface topographies of the screen-printed paper samples

The surface topographical characteristics of both blank and screen-printed papers were examined, and the scanning electron microscopic images captured are shown in Fig. 5. The blank paper displayed a fibrous and porous texture (Fig. 5a), but the print demonstrated an even and smoother surface (Fig. 5b) because the screen print develops a consistent and uniform ink film on the porous substrate. The formation of a uniform homogenous ink film is further supported by the AFM images for blank (Fig. 5c) and printed papers (Fig. 5c) with R_q, R_a, and R_{max} values of 158 nm, 124 nm, and 2003 nm for the unprinted and 119 nm, 97 nm, and 735 nm for the screen-printed paper samples.

Security applications

The BTNP ink which shows an intense yellowish–green UV fluorescence could find potential applications in anticounterfeiting, automatic identification, and data security. Moreover, the biocompatibility of the chalcone-derived water-based ink enables its usage as an alternative to the traditional inks in thumbprint inkpads and stamp pads, which is an effective and simple technique to allow the safety of security documents against fraud. The BTNP ink on cost-effective, recyclable, eco-friendly, and flexible paper substrates could also be explored for printed technologies in electronic anticounterfeiting including RFIDs, wherein genuine products/items can be identified and tracked. The water-based ink can also be used to add more security features as labels or in packaging against fraudulent replication.

Conclusion

The preparation of a bithiophene-naphthalene chalcone BTNP for potential usage as a colourant in the formulation of a water-based UV fluorescent screen-printing ink, which could expand future practical applications is reported in the present study. The pigment synthesized using a simple aldol condensation reaction showed aggregation-induced emission and intramolecular charge transfer features. The UV fluorescent screen prints exhibited fast drying, good adhesion, light

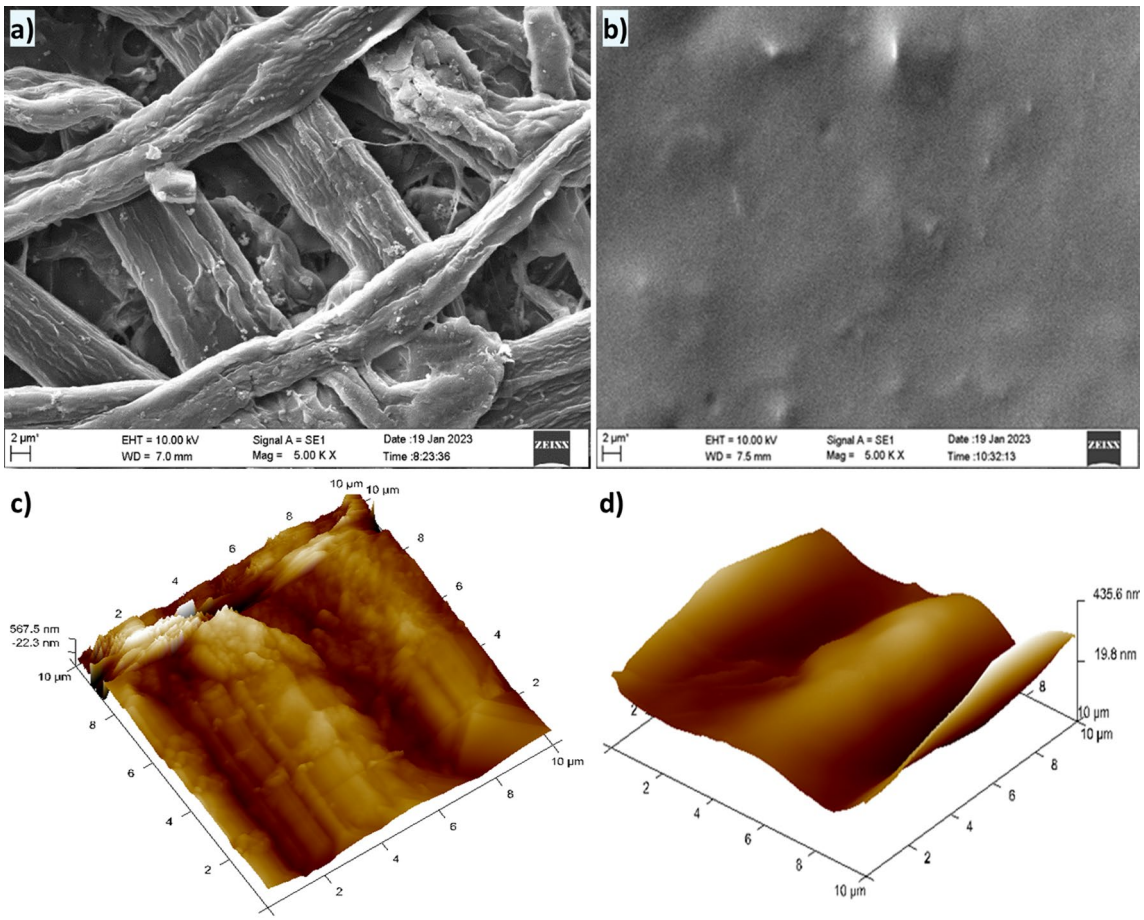

Fig. 5 SEM images of **a** blank and **b** screen-printed and AFM images of **c** blank and **d** screen-printed UV dull paper samples

stability, and rub resistance on porous paper substrate. The eco-friendly ink can find potential applications in diverse fields including data security, inkpads, and in electronic anti-counterfeiting for product tracking and identification. Moreover, the BTNP ink being environment-friendly and less toxic can be used in the labelling and packaging industry.

Supplementary Information The online version contains supplementary material available at https://doi.org/10.1007/s11696-023-02958-2.

Funding Open access funding provided by Manipal Academy of Higher Education, Manipal.

Data availability The data are available upon reasonable request from RKJ (rakshithajain710@gmail.com) and KM (kashmithakc@gmail.com).

Declarations

Conflict of interest The authors declare no conflict of interest with this work.

References

Abdollahi A, Roghani-Mamaqani H, Razavi B, Salami-Kalajahi M (2020) Photoluminescent and chromic nanomaterials for anticounterfeiting technologies: recent advances and future challenges. ACS Nano 14:14417–14492. https://doi.org/10.1021/acsnano.0c07289

Al-Ansari IAZ (2016) Physicochemical properties of derivatives of *N, N*- dimethylamino-cyclic-chalcones: experimental and theoretical study. ChemistrySelect 1:2935–2944. https://doi.org/10.1002/slct.201600458

Ataeefard M, Nourmohammadian F (2015) Producing fluorescent digital printing ink: Investigating the effect of type and amount of coumarin derivative dyes on the quality of ink. J Lumin 167:254–260. https://doi.org/10.1016/j.jlumin.2015.06.042

Barbarella G, Melucci M, Sotgiu G (2005) The versatile thiophene: an overview of recent research on thiophene-based materials. Adv Mater 17:1581–1593. https://doi.org/10.1002/adma.200402020

Bhagya RS, Sunil D, Muthamma K et al (2022) Water-based invisible green flexographic ink for anti-counterfeit applications. Prog Org Coat 173:107212. https://doi.org/10.1016/j.porgcoat.2022.107212

Gulyani A, Dey N, Bhattacharya S (2018) Tunable emission from fluorescent organic nanoparticles in water: insight into the nature of self-assembly and photoswitching. Chem - Eur J 24:2643–2652. https://doi.org/10.1002/chem.201704607

Ibrar M, Skrabalak SE (2021) Designer plasmonic nanostructures for unclonable anticounterfeit tags. Small Struct 2:2100043. https://doi.org/10.1002/sstr.202100043

Jeon S, Lee JP, Kim J-M (2015) In situ synthesis of stimulus-responsive luminescent organic materials using a reactive inkjet printing approach. J Mater Chem C 3:2732–2736. https://doi.org/10.1039/C5TC00334B

Jiang K, Wang Y, Cai C, Lin H (2018) Conversion of carbon dots from fluorescence to ultralong room-temperature phosphorescence by heating for security applications. Adv Mater 30:1800783. https://doi.org/10.1002/adma.201800783

Kagatikar S, Sunil D (2021) Aggregation induced emission of chalcones. Chem Pap 75:6147–6156. https://doi.org/10.1007/s11696-021-01793-7

Karuppusamy A, Vandana T, Kannan P (2017) Pyrene based chalcone materials as solid state luminogens with aggregation-induced enhanced emission properties. J Photochem Photobiol Chem 345:11–20. https://doi.org/10.1016/j.jphotochem.2017.05.026

Kim Y-S, Son Y-A (2011) Synthesis of 2,2-bithiophene based dye sensor and optical properties toward metal cations. Mol Cryst Liq Cryst 551:163–171. https://doi.org/10.1080/15421406.2011.600640

Lakowicz JR (1983) Principles of Fluorescence Spectroscopy. Springer, US, Boston, MA

Leach RH, Armstrong C, Brown JF et al (eds) (1988) The Printing Ink Manual, 4th edn. Springer, Netherlands, Dordrecht

Lee SC, Lee M, Suh B et al (2021) A Bithiophene-based Ratiometric Fluorescent Sensor for Sensing Cd $^{2+}$. ChemistrySelect 6:8397–8401. https://doi.org/10.1002/slct.202102503

Li J, Xia D, Gao M et al (2021) Invisible luminescent inks and luminescent films based on lanthanides for anti-counterfeiting. Inorganica Chim Acta 526:120541. https://doi.org/10.1016/j.ica.2021.120541

Mieno H, Kabe R, Adachi C (2018) Reversible control of triplet dynamics in metal-organic framework-entrapped organic emitters via external gases. Commun Chem 1:27. https://doi.org/10.1038/s42004-018-0027-x

Ming LS, Jamalis J, Al-Maqtari HM et al (2017) Synthesis, characterization, antifungal activities and crystal structure of thiophene-based heterocyclic chalcones. Chem Data Collect 9–10:104–113. https://doi.org/10.1016/j.cdc.2017.04.004

Mortimer RJ, Varley TS (2011) Quantification of colour stimuli through the calculation of CIE chromaticity coordinates and luminance data for application to in situ colorimetry studies of electrochromic materials. Displays 32:35–44. https://doi.org/10.1016/j.displa.2010.10.001

Muthamma K, Sunil D, Shetty P et al (2021) Eco-friendly flexographic ink from fluorene-based Schiff base pigment for anti-counterfeiting and printed electronics applications. Prog Org Coat 161:106463. https://doi.org/10.1016/j.porgcoat.2021.106463

Muthamma K, Gouda BM, Sunil D et al (2023) Water-based fluorescent flexo-ink for security applications. Chem Pap. https://doi.org/10.1007/s11696-023-02765-9

Omar S, Mohd S, AlFaify S et al (2018) Molecular structure, vibrational, optical and second order polarizabilities of (E)-1-(2′,4′-Dihydroxy-phenyl)-3-(2,3-dimethoxyphenyl)-propenone chalcone derivative: a quantum computational approach. Opt Quantum Electron 50:278. https://doi.org/10.1007/s11082-018-1540-y

Pei K, Zhou H, Yin Y et al (2020) Highly fluorescence emissive 5, 5′-distyryl-3, 3′-bithiophenes: Synthesis, crystal structure, optoelectronic and thermal properties. Dyes Pigments 179:108396. https://doi.org/10.1016/j.dyepig.2020.108396

Rasmussen SC, Evenson SJ, McCausland CB (2015) Fluorescent thiophene-based materials and their outlook for emissive applications. Chem Commun 51:4528–4543. https://doi.org/10.1039/C4CC09206F

Samanta SK, Bhattacharya S (2012) Aggregation induced emission switching and electrical properties of chain length dependent π-gels derived from phenylenedivinylene bis-pyridinium salts in alcohol–water mixtures. J Mater Chem 22:25277. https://doi.org/10.1039/c2jm35012b

Song Z, Lin T, Lin L et al (2016) Invisible Security Ink Based on Water-Soluble Graphitic Carbon Nitride Quantum Dots. Angew Chem Int Ed 55:2773–2777. https://doi.org/10.1002/anie.201510945

Sowmiya M, Tiwari AK, Sonu SSK (2011) Study on intramolecular charge transfer fluorescence properties of trans-4-[4′-(N, N′-dimethylamino)styryl]pyridine: Effect of solvent and pH. J Photochem Photobiol Chem 218:76–86. https://doi.org/10.1016/j.jphotochem.2010.12.006

Venkateswarlu S, Reddy AS, Panda A et al (2020) Reversible fluorescence switching of metal-organic framework nanoparticles for use as security ink and detection of Pb^{2+} ions in aqueous media. ACS Appl Nano Mater 3:3684–3692. https://doi.org/10.1021/acsanm.0c00392

Wakamiya A, Mori K, Yamaguchi S (2007) 3-Boryl-2,2′-bithiophene as a versatile core skeleton for full-color highly emissive organic solids. Angew Chem 119:4351–4354. https://doi.org/10.1002/ange.200604935

Zhou X, Li Y, Fang C et al (2015) Recent advances in synthesis of waterborne polyurethane and their application in water-based ink: a review. J Mater Sci Technol 31:708–722. https://doi.org/10.1016/j.jmst.2015.03.002

Żołek-Tryznowska Z, Izdebska J, Tryznowski M (2015) Branched polyglycerols as performance additives for water-based flexographic printing inks. Prog Org Coat 78:334–339. https://doi.org/10.1016/j.porgcoat.2014.07.015

Authors and Affiliations

Rakshitha K. Jain[1] · Kashmitha Muthamma[1] · Dhanya Sunil[1] · Suresh D. Kulkarni[2] · P. J. Anand[3] · Nilanjan Dey[4]

✉ Dhanya Sunil
dhanyadss3@gmail.com

[1] Department of Chemistry, Manipal Institute of Technology, Manipal Academy of Higher Education, Manipal, Karnataka 576104, India

[2] Department of Atomic and Molecular Physics, Manipal Academy of Higher Education, Manipal, Karnataka 576104, India

[3] Manipal Technologies Limited, Manipal, Karnataka 576104, India

[4] Department of Chemistry, Birla Institute of Technology and Science Pilani, Hyderabad Campus, Secunderabad, Telangana 500078, India